



Antibacterial Activity of Free and Liposome-Encapsulated Tylosin Against Planktonic and Biofilm Forms of *Corynebacterium pseudotuberculosis* Isolated from Goats

MohammadEhsan SADDIQI^{1,2} , Arifah ABDUL KADIR¹ 

¹Department of Veterinary Preclinical Studies, Faculty of Veterinary Medicine, Universiti Putra Malaysia, Serdang, Selangor, Malaysia

²Department of Clinic, Faculty of Veterinary Science, Herat University, Herat, Afghanistan

Cite this article as: Saddiqi, M. E., & Abdul Kadir, A. (2024). Antibacterial activity of free and liposome-encapsulated tylosin against planktonic and biofilm forms of *Corynebacterium pseudotuberculosis* isolated from goats. *Acta Veterinaria Eurasia*, 50(2), 119-127.

Abstract

Corynebacterium pseudotuberculosis causes infection in goats, sheep, cattle, and humans. The disease imposing huge economic losses such as reducing milk, meat, and wool production and downgrading and condemnation of affected carcass to goat-rearing industry. Despite all its devastating effects, no effective antimicrobial was suggested for the treatment of this pathogen due to its highly resistant nature. Development and utilization of nanoparticles has paved the way to revive the efficacy of conventional antibiotics. Encapsulation of antibiotics within liposome as a nanoparticle may present a potential approach for successful treatment of resistant bacterial infections. The aim of this research was therefore to evaluate the antibacterial activity of free and liposome-encapsulating tylosin against *Corynebacterium pseudotuberculosis*. The minimum inhibitory concentration of free and liposome-encapsulated tylosin was determined by microbroth dilution and resazurin colorimetric-based methods. The antibiofilm activity of free and liposomal tylosin was assessed by crystal

violet and resazurin techniques. Acridine orange/ethidium bromide staining assay was performed to assess the effect of free and liposomal tylosin on pre-formed biofilm of *Corynebacterium pseudotuberculosis*. The findings demonstrated minimum inhibitory concentration value of 1 µg/mL and 32 µg/mL for free and liposomal tylosin, respectively. The biofilm inhibitory data showed that free tylosin inhibited the formation of *Corynebacterium pseudotuberculosis* at 2 µg/mL, while this concentration was 64 µg/mL for liposomal tylosin. The antibiofilm concentration was 1024 µg/mL and 2048 µg/mL for liposome-encapsulated and free tylosin, respectively. It can be concluded that liposome as a nanocarrier can offer an excellent system of drug delivery for enhancing the efficacy of antibiotics against resistant form of *Corynebacterium pseudotuberculosis*.

Keywords: Biofilm, *Corynebacterium pseudotuberculosis*, liposome, planktonic, tylosin

Introduction

Corynebacterium pseudotuberculosis (*C. pseudotuberculosis*) is a Gram-positive, non-spore forming, pleomorphic, facultative anaerobic, facultative intracellular coccobacillus, and non-motile (Corrêa et al., 2018; Latif et al., 2015; Ruiz et al., 2020). The bacterium is the leading cause of caseous lymphadenitis disease in different types of mammalian species and is highly significant in small ruminants, especially in goats and sheep (Galvão et al., 2017; Guerrero et al., 2018). Caseous lymphadenitis is an infectious disease with chronic and subclinical manifestations that spread all around the globe (de Sá Guimarães et al., 2011; Yitagesu et al., 2020). The disease causes huge economic losses such as decreasing production of meat, milk, wool, downgrading, and condemnation of affected carcasses at the meat inspection and slaughterhouse (Aftabuzzaman & Cho, 2021; Burmayer & Brundage, 2021; Schlicher et al., 2021; Stanisic et al., 2018). These devastating effects have driven many researchers toward combating against caseous lymphadenitis. Moreover, global

distribution, contagious property, lack of appropriate and effective control actions (Abebe & Sisay Tessema, 2015), and zoonotic nature of the disease (de Sá Guimarães et al., 2011; Magdy Selim et al., 2021) have introduced the disease as one of the most devastating infections in small ruminant husbandry.

Despite the high prevalence and importance of caseous lymphadenitis, there is no effective and appropriate treatment line for the disease to date (de Pinho et al., 2021; Minozzi et al., 2017). There are some major factors, including encapsulation of the lesion with a thick fibrous capsule (Stanisic et al., 2018) and the intracellular location of the pathogen (Washburn et al., 2009), which limit the availability of an appropriate concentration of antibacterial agents at the site of infection. Therefore, this results in failure of chemotherapy for caseous lymphadenitis infection (de Pinho et al., 2021; Stanisic et al., 2018). Furthermore, the *in vivo* biofilm formation capability of *C. pseudotuberculosis* makes it highly refractory to the effect of many chemotherapeutic agents (Olson et al., 2002; Sá et al., 2013).

Corresponding Author: Arifah ABDUL KADIR • E-mail: arifah@upm.edu.my

Received: October 10, 2023 • **Revision requested:** November 16, 2023 • **Last revision received:** January 16, 2024 • **Accepted:** February 6, 2024 •

Publication Date: April 9, 2024 • DOI: 10.5152/actavet.2024.23070

Available online at actavet.org



This work is licensed under a Creative Commons Attribution-NonCommercial 4.0 International License.

Biofilm formation is one of the best approaches that enables bacteria to escape both from the effects of antibacterial agents and the response of the host immune system (Alhajlan et al., 2013). Therefore, the formation of biofilm possesses a critical concern in the health sector worldwide (Sharma et al., 2019). Biofilm is described as a bacterial aggregation that makes a colony and able to grow either on biotic and abiotic surfaces through their own produced extracellular polymeric substances (EPSs) (Dumaru et al., 2019). The EPSs are comprised of proteins, polysaccharides, nucleic acids, and lipid substances (Rukavina & Vanić, 2016) which delay the penetration of chemotherapeutic agents into the deep site of the biofilms (Alhajlan et al., 2013; Moreau-Marquis et al., 2008). In addition, the electrostatic property donated by the negatively charged extracellular matrix is another important factor that limits the penetration of positively charged antibiotics in biofilm (Alhariri et al., 2017). Considering the abovementioned explanation, infections caused by means of bacterial biofilms are challenging to treat. Therefore, searching for novel approaches to fight against bacterial biofilms is an urgent necessity, hence loading antibiotics within liposomes as a potential nanoparticle for drug delivery can be an option.

The employing of nanoparticles as a carrier system for antibiotics provides a novel approach to control and treat infections caused by resistant organisms (Hallaj-Nezhadi & Hassan, 2015). It has been indicated that the application of nanoparticles increases the efficacy of antibiotics not only against planktonic bacteria but also against biofilm-forming microorganisms (Gupta et al., 2019). Liposomes, as unique nanoparticle plays a crucial role in this regard since they are the most widely used nanocarriers for antimicrobial drugs (Rukavina & Vanić, 2016; Thapa et al., 2021; Zong et al., 2022). Liposomes are described as lipid vesicles with a spherical shape composed of one or more phospholipid bilayers surrounding an aqueous compartment (Drulis-Kawa & Dorotkiewicz-Jach, 2010). Liposomes are able to incorporate a large number of biological materials like antioxidants, DNA, RNA, drugs, and vitamins (Alhariri et al., 2017; Ferreira et al., 2021). Furthermore, their unique properties in the incorporation of both hydrophilic and hydrophobic compounds, as well as their compatibility and biodegradability, have introduced them as the best candidates for antibiotic delivery (Abed & Couvreur, 2014; Wang et al., 2020). Loading antibiotics into liposomes presents an attractive strategy to overcome biofilm problems through effective penetration into biofilms and target sites and sustained release of antibiotics (Alhariri et al., 2017; Kluzek et al., 2022; Meers et al., 2008). Many studies have demonstrated the efficacy of liposomes in improving the antibacterial activity of antibiotics against biofilm-forming pathogens such as amikacin (Meers et al., 2008), clarithromycin (Alhajlan et al., 2013), chloramphenicol (Dias-Souza et al., 2017), gentamicin (Alhariri et al., 2017), and azithromycin (Vanić et al., 2019).

Tylosin is active against a wide variety of microorganisms and belongs to the family of macrolides produced by *Streptomyces fradiae* and commonly used as a drug in veterinary medicine (Ji et al., 2014). Tylosin stops bacterial growth by preventing synthesis of protein through binding to large portion (50s subunit) of the ribosome (Lohsen & Stephens, 2019; Poźniak et al., 2020). The main antimicrobial spectrum of tylosin includes Gram-positive bacteria, however, *Mycoplasma*, some Gram-negative, and anaerobic bacteria are also sensitive to tylosin (Avci & Elmas, 2014; Ji et al., 2014). Over time, inappropriate, overconsumption and usage of antibiotics to prevent

microbial diseases in livestock cause bacterial resistance toward this valuable antibiotic and other macrolides (Gaynor & Mankin, 2003; Lohsen & Stephens, 2019; Poźniak et al., 2020). Resistant bacteria employ a range of tactics, including target site alteration and decreasing cell membrane permeability, to evade the effects of macrolides (Alhajlan et al., 2013). On the other hand, *C. pseudotuberculosis* can readily escape the effects of antibiotics utilizing *in vivo* biofilm formation, which is another important resistance mechanism (Olson et al., 2002). As a result, all the abovementioned factors decrease the antibacterial activity of tylosin in the treatment of infectious diseases.

Although it has been demonstrated that liposomes enhance the antibacterial activity of many loaded antibiotics, no study has been performed to determine the possible potency of liposomes as a nanocarrier to enhance the efficacy of tylosin against *C. pseudotuberculosis*. Therefore, the main purpose of this study is to determine the *in vitro* antibacterial efficacy of free and liposome-encapsulated tylosin against planktonic and biofilm forms of *C. pseudotuberculosis*. To the best of our knowledge, no research has been conducted to figure out the effect of tylosin and liposome-encapsulated tylosin against both planktonic and biofilm forms of *C. pseudotuberculosis* so far.

Materials and Methods

Tylosin tartrate, resazurin sodium salt, acridine orange, ethidium bromide, Phosphate buffered saline tablets, and cholesterol were purchased from Sigma (Sigma-Aldrich, Saint Louis, MO 63103, USA). Egg phosphatidylcholine (EPC) was obtained from Avanti (Avanti Polar Lipids, Inc., Alabaster, Alabama, USA). Tryptone soya broth (TSB) and Mueller Hinton Broth (MHB) were received from Oxoid (Oxoid Ltd, Basingstoke, Hampshire, UK). The analytical grade solvents were used throughout the experiment.

Culture of *Corynebacterium pseudotuberculosis*

C. pseudotuberculosis was obtained from the stock culture (UPMC-894) of the Clinical Diagnosis Laboratory, Faculty of Veterinary Medicine, University Putra Malaysia. The bacterium was cultured for 48 h at 37°C. The staining properties of *C. pseudotuberculosis* were confirmed by the Gram staining method.

Antibacterial Activity Against the Planktonic Bacteria

Empty liposomes and liposome-encapsulated tylosin were prepared as in our previous research (Saddiqi et al., 2022). The minimum inhibitory concentration (MIC) of the free and liposome-encapsulated tylosin formulation against *Corynebacterium pseudotuberculosis* was determined using a microtiter plate assay (microbroth dilution) and resazurin colorimetric-based techniques. In the microdilution method, 100 µL of sterile MHB was added to flat-bottomed 96-well microtiter plates. Afterward, 100 µL of empty liposome, liposome-encapsulated tylosin, and free tylosin, which was prepared in MHB, were added to the first well, and two-fold serial dilution was performed to obtain a concentration range from 128µg/mL to 0.125µg/mL for each treatment. The treatments were not added to the last row to serve as the control. Then, five microliters of an overnight diluted culture of *C. pseudotuberculosis* (approximately 1.0×10^8 cfu/mL) in TSB supplemented with 2% fetal bovine serum (FBS) were added to each treatment row except the control ones. Rows with only MHB served as sterility control. The plates were incubated at 37°C for 24 h. The MIC values were determined by visual turbidity

assessment, and for further confirmation, the absorbance was taken using a Tecan microplate reader (Tecan Infinite M200PRO, Tecan Group Ltd., Männedorf, Switzerland) at a 600 nm wavelength. The lowest concentration that prevented the growth of bacteria (demonstrating no visible growth after 24-hour-incubation period) was considered as the MIC.

The resazurin reduction assay was performed for further accuracy establishment of MIC values against *C. pseudotuberculosis* according to the method described previously (Foerster et al., 2017). The plating of bacterial culture was done as described in the microdilution method. The final concentration of resazurin (0.1 mg/mL) was prepared by dissolving one milligram of resazurin powder in 10 mL of sterile PBS (pH 7.4) and mixed properly by vigorous vortexing. The resazurin solution was sterilized by passing through a Whatman® syringe filter with a 0.2 µm pore size. The 96-well plates containing treatments and bacterial culture as described above were incubated for 24 hours at 37°C. After incubation, 50 µL of the resazurin solution (0.1 mg/mL) was added to each well and incubated at 37°C for further 3 hours. Finally, visually assessment of the wells was done, and the wells with no color change (blue color of resazurin unchanged) were assigned as MIC values. Besides visual evaluation, the fluorescence absorbance was measured using a Tecan microplate reader (Tecan Infinite M200PRO, Tecan Group Ltd., Männedorf, Switzerland) for resazurin and resorufin at 570 and 600 nm, respectively.

Antibacterial Activity Against Biofilm Form of *Corynebacterium pseudotuberculosis*

Quantification of *Corynebacterium pseudotuberculosis* Biofilm

Formation and quantitative determination of *C. pseudotuberculosis* biofilm were performed based on a standard static biofilm assay as described by Alhariri and colleagues (Alhariri et al., 2017). An overnight culture of *C. pseudotuberculosis* was diluted into fresh tryptic soya broth to give an approximate bacterial number of 1.0×10^7 cfu/mL. Two hundred microliters of diluted culture was poured into 96-well plates and incubated in a CO₂ incubator (Binder, Germany) at 37°C for 24 hours in the presence of 10% CO₂ to assess biofilm formation. Then, the 96-well plate contains were discarded to remove the media and unattached *C. pseudotuberculosis* and were rinsed three times with sterile distilled water to remove the remaining media and unattached bacteria. After that, two hundred microliters of 0.1% crystal violet solution was added to each well of the 96-well plate to evaluate the *C. pseudotuberculosis* biofilm biomass and the plates were kept for 15 minutes at room temperature. The plates were washed gently three times to discard the extra crystal violet and were dried completely by keeping them upside down on tissue paper overnight. To determine the formed biofilm biomass, 200 µL of 30% acetic acid was added to solubilize the incorporated crystal violet and the plates were maintained for 15 min at room temperature. The solubilized crystal violet was then transferred into a new 96-well microtiter plate. The biofilm biomass was quantified by taking the absorbance of the solubilized crystal violet using a Tecan microplate reader (Tecan Infinite M200PRO, Tecan Group Ltd., Männedorf, Switzerland) at a wavelength of 600 nm, and 30% acetic acid in sterile distilled water was used as the blank. The experiment was performed three times independently on different days. The mean of the optical density (OD) at 600 nm was calculated. The interpretation of results was done as follows: positive (>0.24); weak (>0.12 and <0.24) and negative (<0.12) (Qin et al., 2014). These values represent the amount of crystal violet taken by the biofilm-producing strains.

Therefore, strong biofilm-producers will have a high OD of (>0.24), while weak and non-biofilm-producers will indicate OD of (>0.12 and <0.24) and (<0.12), respectively (Arciola et al., 2006; Christensen et al., 1985; Qin et al., 2014).

Determination of the Minimum Biofilm Eradication Concentration of Free and Liposome-Encapsulated Tylosin

Minimum biofilm eradication concentration of liposome-encapsulated tylosin, empty liposome, and free tylosin against *C. pseudotuberculosis* was performed based on the previous method (Mulla et al., 2016; Sherifat et al., 2021). Overnight culture of *C. pseudotuberculosis* in tryptic soya broth supplemented with 2% FBS was diluted into fresh MHB supplemented with 2% FBS, which was given approximately 1×10^7 cfu/mL in sterile glass tubes. Afterwards, 200 µL of diluted *C. pseudotuberculosis* culture was poured into each well of the 96-well microtiter plates and incubated for 24 hours at 37°C in the presence of 10% CO₂. Crystal violet (0.1%) staining of the 96-well microtiter plates for 15 minutes was performed to confirm the formation of *C. pseudotuberculosis* biofilm. After 15 minutes, crystal violet was decanted and the plates were gently submerged in water and shaken out to remove the excess crystal violet from the wells, and further blotted dry on towel paper. The formed biofilms were exposed to different concentrations ranging between 2048 µg/mL and 1 µg/mL of liposome-encapsulated tylosin, empty liposome, and free tylosin and incubated at 37°C for 24 hours. The minimum biofilm eradication concentration (MBEC) was determined by visually evaluating the plate's turbidity and further confirmed by taking the absorbance at 600 nm using a Tecan microtiter plate reader (Tecan Infinite M200PRO, Männedorf, Switzerland) as explained by Harrison (Harrison et al., 2006). An optical density of <0.1 was considered as the MBEC (Harrison et al., 2006).

Corynebacterium pseudotuberculosis Biofilm Inhibition Assessment

The current experiment was performed to evaluate the efficacy of liposome-encapsulated tylosin, and free tylosin in preventing *in vitro* biofilm formation by *C. pseudotuberculosis*. Therefore, two methods, crystal violet staining and resazurin-based colorimetric assay, were applied to determine the minimum biofilm inhibitory concentration (MBIC) of both liposome-encapsulated tylosin and free tylosin.

Crystal Violet Staining

The biofilm inhibitory activity of free and liposome-encapsulated tylosin against *C. pseudotuberculosis* was evaluated based on crystal violet staining assay as described by (Goel & Mishra, 2018; Sherifat et al., 2021). Hundred µL of a diluted overnight culture of *C. pseudotuberculosis* into fresh tryptic soya broth which was given an approximate bacterial number of 1×10^7 cfu/mL, was added to wells of non-tissue culture treated 96-well microtiter plates with different concentrations of free and liposome-encapsulated tylosin varying from 1 µg/mL to 256 µg/mL prepared by two-fold serial dilution in MHB and incubated at 37°C for 24 hours with 10% CO₂. The untreated wells served as the control. Once the incubation period is completed, the treated and untreated wells were decanted and washed with sterile PBS to confirm the complete removal of unattached or planktonic *C. pseudotuberculosis*. Afterward, each well was filled with 200 µL of 0.1% crystal violet solution and kept for 15 minutes at room temperature. The crystal violet solution was removed from the wells, and sterile phosphate-buffered saline was used to rinse the excess crystal violet three times. To dissolve the incorporated crystal violet,

30% acetic acid was added to each well of the 96-well plates and incubated at room temperature for 15 minutes. Finally, the unincorporated crystal violet was transferred to a new flat-bottomed 96-well microtiter plate, and the absorbance was taken at 600 nm spectrophotometrically using Tecan microtiter plate reader (Tecan Infinite M200PRO, Männedorf, Switzerland). The biofilm inhibition percentage was calculated using the following equation:

$$\text{Percentage of Biofilm Inhibition} = \frac{\text{Control Absorbance} - \text{Sample Absorbance}}{\text{Control Absorbance}} \times 100\%$$

Resazurin-Based Assay

The procedure for plating the bacteria into a 96-well plate and exposing them to various concentrations of liposome-encapsulated tylosin and free tylosin was done the same as described for the crystal violet staining method as mentioned above. Following treatment of bacterial culture with various concentrations (1 µg/mL to 256 µg/mL) and incubated for 24 hours at 37°C in the presence of 10% CO₂, the media with treatment was removed from the wells and the wells were rinsed three times with sterile PBS. Afterwards, resazurin (0.02%) was added to each well and further incubated for 4 hours at 37°C. Once the incubation is completed, the fluorescence was taken by the Tecan microtiter plate reader (Tecan Infinite M200PRO, Männedorf, Switzerland) at a wavelength of 570 nm to 600 nm, which was set for fluorescence adjustment. The current formula was applied to measure the biofilm inhibition percentage, wherein the formula FluoreAbs indicate the fluorescence absorbance.

$$\text{Percentage of Biofilm Inhibition} = \frac{\text{FluoreAbs of Control} - \text{FluoreAbs of Samples}}{\text{FluoreAbs of Control}}$$

Live/Dead Assessment of *Corynebacterium pseudotuberculosis* Biofilm

The antibiofilm effect of free and liposome-encapsulated tylosin formulations was evaluated on *C. pseudotuberculosis* pre-formed biofilm based on a previous method (Sherifat et al., 2021). The *C. pseudotuberculosis* biofilm was treated with the MBEC concentration of free and liposome-encapsulated tylosin and incubated at 37°C for 24 hours. The plates containing biofilm with media served as control throughout the study. Following the incubation, the control and treated biofilm plates were washed with sterile PBS three times. Afterwards, the plates were stained with 6 µl of acridine orange (fluoresces green is used for live cells staining)/ethidium bromide (fluoresces red and is used for staining of dead cells) (100 µg/mL and 3000 µg/mL, respectively) and further incubated in the dark for 20 minutes at room temperature. Then, the excess stain was eliminated from each well and the wells were observed under the fluorescent microscope (Nikon/TI-S, Japan) and photographed with the fluorescein isothiocyanate (FITC) filter (green) for viable cells and the tetramethylrhodamine isothiocyanate (TRITC) filter (red) for dead cells, as explained previously (Skogman et al., 2016).

Statistical Analysis

The data analysis was performed statistically using GraphPad Prism (version 8.0.2) software package. Two-way analysis of variance test with Tukey's post hoc test was applied for comparisons of the control and experimental group means. Data was considered statistically

significant when the *p*-value was less than .05 (*p* < .05). All experiments were conducted in triplicates and the mean ± SD was used to express the results.

Results

In vitro Antimicrobial Activity of Free and Liposome-Encapsulated Tylosin

The MIC and MBEC of liposome-encapsulated tylosin were evaluated against both planktonic and biofilm forms of *C. pseudotuberculosis*. The ratio of 2:1 of egg phosphatidylcholine: cholesterol was used to prepare empty liposomes that showed no antibacterial activity against the bacteria. The MIC and MBEC values of free and liposome-encapsulated tylosin are summarized in Table 1. As indicated in Table 1, the liposome-encapsulated tylosin, and free tylosin inhibit the growth of *C. pseudotuberculosis* at 32 µg/mL and 1 µg/mL, respectively. In contrast, liposome-encapsulated tylosin indicated better antibiofilm activity and eradicated the *C. pseudotuberculosis* biofilm at a concentration of 1024 µg/mL, whereas this concentration was 2048 µg/mL for free tylosin. The MIC results were further confirmed by the resazurin-based microplate approach (Figure 1). In this technique, the resazurin added to sterility control wells showed no change in color and remained blue, indicating no contamination had occurred during the experiments, while the resazurin added to the positive control wells completely changed to its reduced form resorufin with a pink color. Wells containing empty liposomes, liposome-encapsulated tylosin, and free tylosin indicated a different degree of resazurin color change. The MIC values were determined where there were no changes in resazurin color in the treatment wells.

Biofilm Inhibitory Activity of Free and Liposome-Encapsulated Tylosin

The results achieved from *C. pseudotuberculosis* biofilm inhibitory assay indicated that both free and liposome-encapsulated tylosin were able to prevent the formation of biofilm. However, free tylosin inhibited the biofilm formation more effectively than the liposome-encapsulated tylosin. Crystal violet staining findings demonstrated that free tylosin significantly prevented the formation of biofilm at 2 µg/mL and higher concentrations (*p* < .001) whereas liposome-encapsulated tylosin reduced the formation of biofilm significantly at 64 µg/mL and higher concentrations (*p* < .01) (Figure 2 & 3, respectively). These findings were further confirmed by the resazurin-based colorimetric method. The results obtained from the resazurin method further ascertained the crystal violet results that free and liposome-encapsulated tylosin inhibited the biofilm formation significantly at 2 µg/mL and 64 µg/mL (*p* < .001), respectively (Figure 4 & 5).

Table 1.

Minimum Inhibitory Concentration and Minimum Biofilm Eradication Concentration Values of Liposomal and Free Tylosin Against Planktonic and Biofilm Forms of Corynebacterium pseudotuberculosis

Liposomal Formulations	MIC (µg/mL)	MBEC (µg/mL)
Tylosin Loaded Liposome	32	1024
Free Tylosin	1	2048

MBEC, minimum biofilm eradication concentration; MIC, minimum inhibitory concentration.

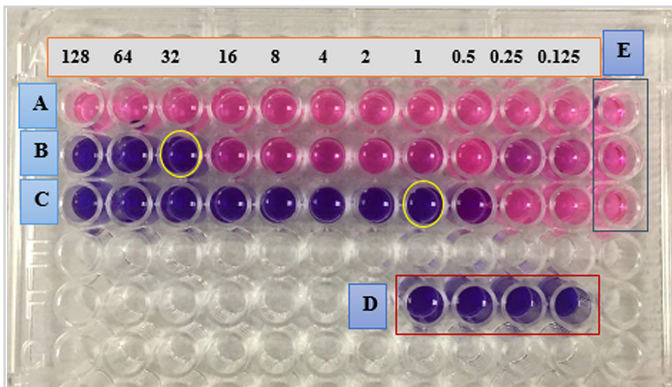


Figure 1.

Minimum inhibitory concentration values of empty liposome, liposome-encapsulated tylosin, and free tylosin against *Corynebacterium pseudotuberculosis* by resazurin-based microplate assay. Following incubation of 24 hours with treatments and 3 hours with resazurin, wells with blue color show dead or inactive bacteria, and wells with pink color indicate live bacteria. The plate contains (A) empty liposome, (B) liposome-encapsulated tylosin, (C) free tylosin, (D) sterility control, and (E) positive control. All treatments were serially diluted with the highest concentration of 128 µg/mL and the lowest concentration of 0.125 µg/mL. The sterility control wells demonstrate no contamination, and the wells containing treatment with no color changes (yellow circles) were considered as MIC values. Empty liposomes exert no antibacterial activity.

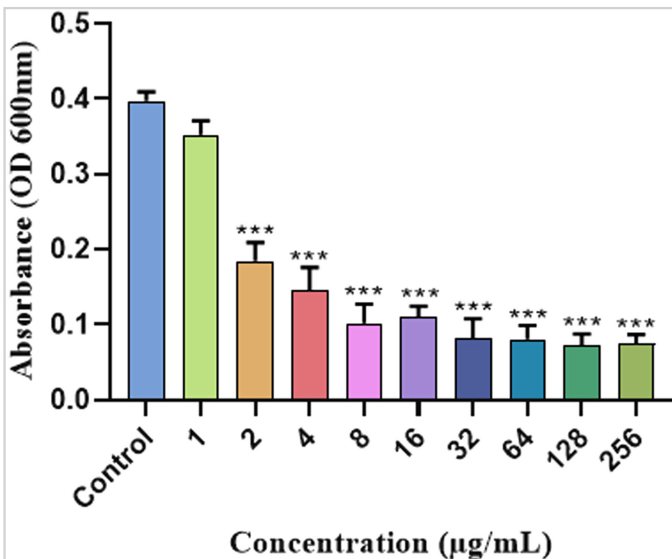


Figure 2.

Inhibitory efficacy of free tylosin on *Corynebacterium pseudotuberculosis* biofilm formation. Mean (\pm SD) optical density values of *C. pseudotuberculosis* biofilms treated with different concentrations of free tylosin based on crystal violet staining method. *** indicates statistically significant difference between the treatments and their untreated control at significance level ($p < .001$).

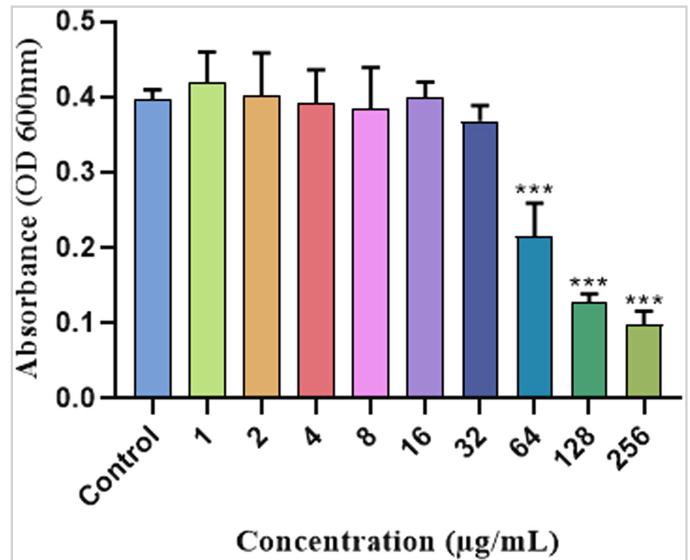


Figure 3.

Inhibitory efficacy of liposome-encapsulated tylosin on *Corynebacterium pseudotuberculosis* biofilm formation. Mean (\pm SD) optical density values of *C. pseudotuberculosis* biofilms treated with different concentrations of liposome-encapsulated tylosin based on crystal violet staining method. *** indicates statistically significant difference between the treatments and their untreated control at significance level ($p < .001$).

Effect of Free and Liposome-Encapsulated Tylosin on Biofilm

Fluorescent imaging of *C. pseudotuberculosis* biofilm treated with liposome-encapsulated tylosin and free tylosin stained with acridine orange (stain viable cells) and ethidium bromide (stain dead cells) was performed to distinguish visually between live and dead biofilm populations based on the integrity of the bacterial cell membrane. Figure 4 indicates the distribution of the live/dead biofilm population following treatment with MBEC concentration of free and liposome-encapsulated tylosin formulations. Figure 6 represents the untreated biofilm, which appears predominantly as viable bacterial cells in green fluorescence. As illustrated in Figure 8, biofilm treated with empty liposomes showed green fluorescence, which is an indicator of a viable biofilm. On the other hand, exposure of the biofilm to free and liposome-encapsulated tylosin showed dead bacterial cells (red fluorescence) and apoptotic bacterial cells (orange-red fluorescence). The biofilm treated with free tylosin showed fewer viable cells (green), apoptotic biofilm population (orange-red), and dead bacterial cells (red) (Figure 7), whereas the biofilm treated with liposome-encapsulated tylosin represented a higher dead bacterial cells (red fluorescence) and apoptotic bacterial cells (yellow and orange-red fluorescence), and fewer viable cells (Figure 9).

Discussion

The antibacterial activity of free and liposome-encapsulated tylosin were evaluated using microbroth dilution and resazurin-based microplate assays, which provide rapid and high-throughput options for determining the antibacterial activity. The resazurin-based microplate assay is a promising approach for assessing the antimicrobial efficacy of antibiotics as it provides many advantages,

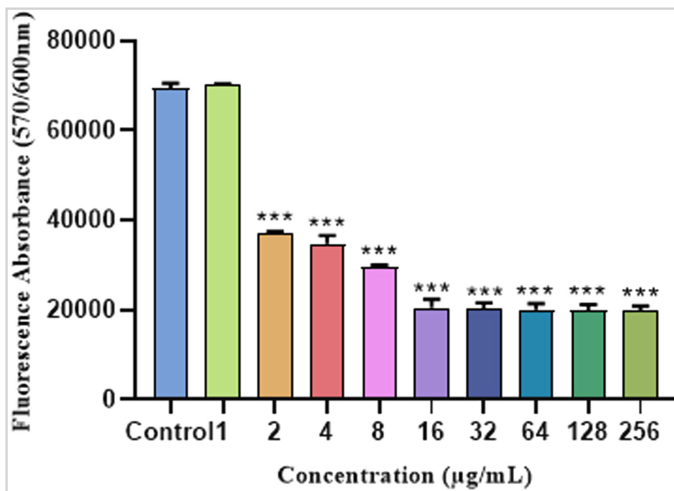


Figure 4.

Inhibitory efficacy of free tylosin on *Corynebacterium pseudotuberculosis* biofilm formation. Mean (\pm SD) optical density values of *C. pseudotuberculosis* biofilms treated with different concentrations of free tylosin based on resazurin-based colorimetric technique. *** indicates statistically significant difference between the treatments and their untreated control at significance level ($p < .001$).

including quick performance, objectivity, lower cost, nontoxic and quantifiability (Foerster et al., 2017). Therefore, in this study, we used both the microdilution technique and the resazurin-based microplate assay to evaluate the *in vitro* antibacterial activity of empty liposomes, liposome-encapsulated tylosin, and free tylosin against *C. pseudotuberculosis*.

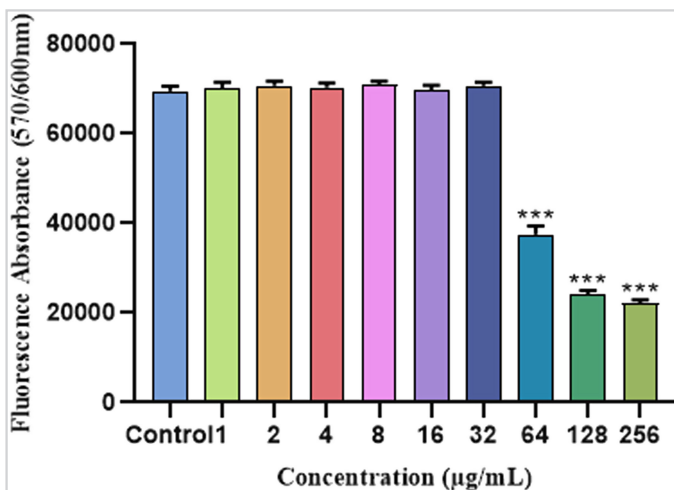


Figure 5.

Inhibitory efficacy of liposome-encapsulated tylosin on *Corynebacterium pseudotuberculosis* biofilm formation. Mean (\pm SD) optical density values of *C. pseudotuberculosis* biofilms treated with different concentrations of liposome-encapsulated tylosin based on resazurin-based colorimetric technique. *** indicates statistically significant difference between the treatments and their untreated control at significance level ($p < .001$).

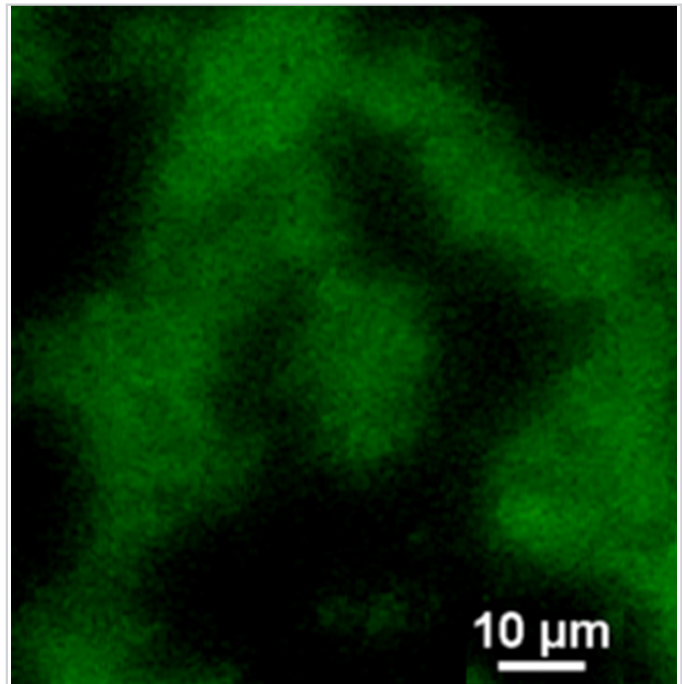
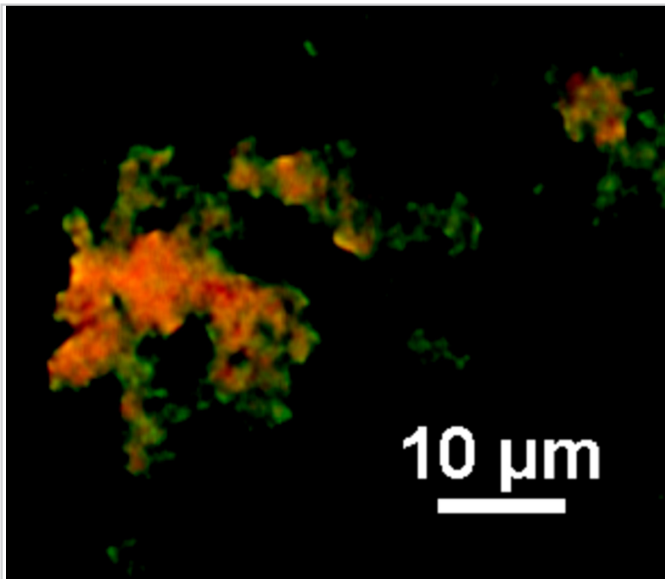


Figure 6.

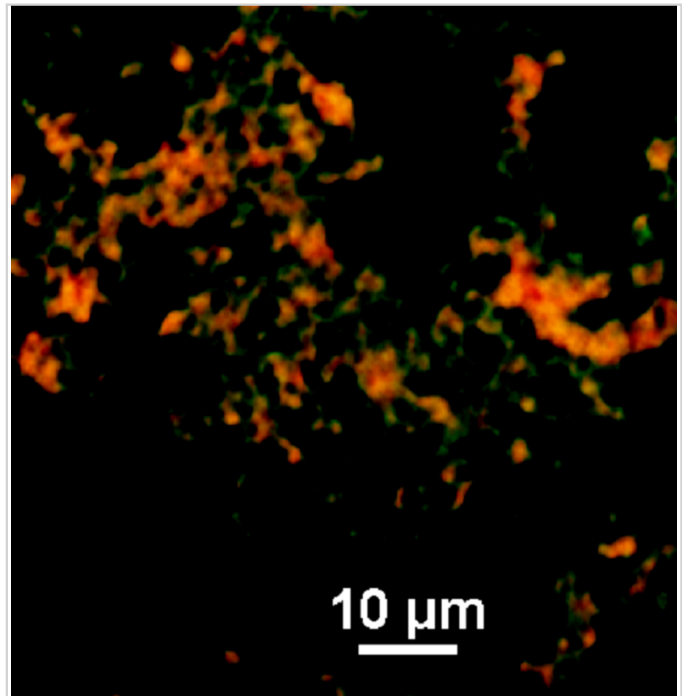
Live/dead assessment of *Corynebacterium pseudotuberculosis* biofilm control group. The green color indicates live biofilm population.

As revealed from the results, the liposome-encapsulated tylosin was unable to enhance the antibacterial activity of free tylosin and exhibited lower activity against the planktonic form of *C. pseudotuberculosis*. For instance, the minimum inhibitory concentration value for liposome-encapsulated tylosin was 32 µg/mL, whereas the MIC value of 1 µg/mL was demonstrated for free tylosin, which is much lower compared to its liposome-encapsulated form. The possible explanation for the lower efficacy of liposome-encapsulated tylosin compared to free tylosin might be because of the bilayer properties of the liposome, which causes less availability of tylosin by hindering its effective release from the liposomes and susceptibility of *C. pseudotuberculosis* to liposome-encapsulated tylosin (Vanić et al., 2019). Our results are in agreement with the research findings performed by Vanić and colleagues indicating that encapsulation of azithromycin into liposomes mainly composed of EPC was unable not only to increase the efficacy of liposome-encapsulated azithromycin but also reduce its antibacterial efficacy (Vanić et al., 2019).

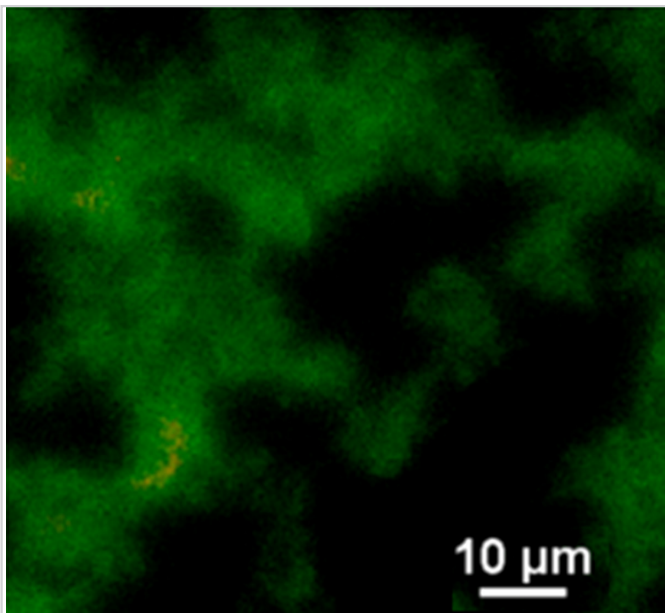
The MBIC findings indicate that both free and liposome-encapsulated tylosin were able to inhibit the formation of biofilm by *C. pseudotuberculosis*. However, free tylosin prevented the formation of biofilm more effectively and at a lower concentration than its encapsulated form. For instance, free tylosin inhibited biofilm formation at 2 µg/mL and higher concentrations, while liposome-encapsulated tylosin inhibited biofilm formation at 64 µg/mL and higher concentrations. The lower biofilm inhibitory efficacy of liposome-encapsulated tylosin may probably come from less availability of tylosin in the environment to interact with the bacterial cells and prevent biofilm formation as a result of antibiotic encapsulation within the liposomes. These results are in line with previous research that demonstrated that free vancomycin inhibited *Staphylococcus aureus*

**Figure 7.**

Live/dead assessment of *Corynebacterium pseudotuberculosis* biofilm following treatment with minimum biofilm eradication concentration concentrations of free tylosin based on the acridine orange/ethidium bromide staining method. The green color indicates the live biofilm population, while red color shows the dead biofilm, and the yellow and orange-red color are indicators of the apoptotic biofilm population.

**Figure 9.**

Live/dead assessment of *Corynebacterium pseudotuberculosis* biofilm following treatment with minimum biofilm eradication concentration concentrations of liposome-encapsulated tylosin based on the acridine orange/ethidium bromide staining method. The green color indicates the live biofilm population, while red color shows the dead biofilm, and the yellow and orange-red color are indicators of the apoptotic biofilm population.

**Figure 8.**

Live/dead assessment of *Corynebacterium pseudotuberculosis* biofilm following treatment with minimum biofilm eradication concentration concentrations of empty liposomes based on acridine orange/ethidium bromide staining method. The green color indicates the live biofilm population, while orange-red color is an indicator of apoptotic biofilm population.

biofilm formation more effectively than its liposome-encapsulated formulation (Scriboni et al., 2019). Conversely, liposome-encapsulated tylosin showed better antibiofilm activity against pre-formed *C. pseudotuberculosis* biofilm compared to free tylosin. For example, the MBEC of liposome-encapsulated tylosin was 1024 $\mu\text{g/mL}$, whereas it was 2048 $\mu\text{g/mL}$ for free tylosin. The enhanced antibiofilm activity of liposome-encapsulated tylosin against pre-formed *C. pseudotuberculosis* biofilm could be due to higher penetration and retention of liposome-encapsulated tylosin in the biofilm. These findings are in agreement with the study indicating that liposome-encapsulated amikacin showed more effective antibiofilm activity against *Mycobacterium avium* biofilm compared to free amikacin (Zhang et al., 2018).

The fluorescent microscopy imaging was used to further validate the MBEC values against *C. pseudotuberculosis* biofilm. The liposome-encapsulated tylosin exerts a profound effect on the pre-formed biofilm of *C. pseudotuberculosis*. The biofilm of *C. pseudotuberculosis* in the control and empty liposomes treated groups emitted green fluorescence predominantly, which is an indicator for viable bacterial cells in the biofilm. The biofilm treated with liposome-encapsulated tylosin displays redder and orange-red fluorescence (dead and apoptotic cells, respectively) than green fluorescence (live cells), indicating more antibiofilm activity of this formulation. On the other side, the biofilm treated with free tylosin shows less red fluorescence compared with the liposomal formulation. Furthermore, free tylosin

appears to be effective on the superficial layer of the biofilm and was not able to diffuse into the deeper part of the biofilm. This may be due to the electrostatic interaction of positively charged tylosin with the negatively charged biofilm matrix, leading to less penetration of free tylosin into the central area of the *C. pseudotuberculosis* biofilm. Overall, the fluorescent microscopy data indicate that liposome as a nanocarrier enhances the efficacy of tylosin against the biofilm resistance form of *C. pseudotuberculosis* and further validates the MBEC values.

To the best of our knowledge, the current study is the first to evaluate the possible efficacy of liposome-encapsulated tylosin against *C. pseudotuberculosis* that causes caseous lymphadenitis. In this study, lipids such as EPC and cholesterol were used for production of liposomes, and tylosin was successfully loaded within them. It was demonstrated that encapsulation of tylosin into liposomes enhanced its antibacterial activity against *C. pseudotuberculosis* biofilm. However, free tylosin indicated better antibacterial activity against the planktonic form of *C. pseudotuberculosis* as compared to liposome-encapsulated tylosin. Therefore, it can be concluded that liposome as nanoparticles may present a potential drug carrying system for enhancing the efficacy of antibiotics against *C. pseudotuberculosis*.

Ethics Committee Approval: Our research did not involve any animal studies and was performed *in vitro* without any experimental animals; therefore, an ethics committee approval is not required.

Peer-review: Externally peer-reviewed.

Author Contributions: Conceptualization – M.E.S., A.A.K.; Methodology – M.E.S.; Software – M.E.S.; Validation – M.E.S., A.A.K.; Formal Analysis – M.E.S.; Investigation – M.E.S., A.A.K.; Resources – M.E.S.; Data Curation – M.E.S.; Writing – Review and Editing – M.E.S., A.A.K.; Visualization – M.E.S., A.A.K.; Supervision – M.E.S., A.A.K.; Project Administration – A.A.K.; Funding Acquisition – A.A.K.

Declaration of Interests: The authors have no conflict of interest to declare.

Funding: This research project was supported by Geran IPS, Universiti Putra Malaysia (Grant No: GP-IPS/2021/9697400).

Data Availability Statement: The corresponding author will provide the data used in this study upon request.

References

- Abebe, D., & Sisay Tessema, T. (2015). Determination of *Corynebacterium pseudotuberculosis* prevalence and antimicrobial susceptibility pattern of isolates from lymph nodes of sheep and goats at an organic export abattoir, Modjo, Ethiopia. *Letters in Applied Microbiology*, 61(5), 469–476. [\[CrossRef\]](#)
- Abed, N., & Couvreur, P. (2014). Nanocarriers for antibiotics: A promising solution to treat intracellular bacterial infections. *International Journal of Antimicrobial Agents*, 43(6), 485–496. [\[CrossRef\]](#)
- Aftabuzzaman, M., & Cho, Y. (2021). Recent perspectives on caseous lymphadenitis caused by *Corynebacterium pseudotuberculosis* in goats-A review. *Korean Journal of Veterinary Service*, 44(2), 61–71. [\[CrossRef\]](#)
- Alhajlan, M., Alhariri, M., & Omri, A. (2013). Efficacy and safety of liposomal clarithromycin and its effect on *Pseudomonas aeruginosa* virulence factors. *Antimicrobial Agents and Chemotherapy*, 57(6), 2694–2704. [\[CrossRef\]](#)
- Alhariri, M., Majrashi, M. A., Bahkali, A. H., Almajed, F. S., Azghani, A. O., Khiyami, M. A., Alyamani, E. J., Aljohani, S. M., & Halwani, M. A. (2017). Efficacy of neutral and negatively charged liposome-loaded gentamicin on planktonic bacteria and biofilm communities. *International Journal of Nanomedicine*, 12(18), 6949–6961. [\[CrossRef\]](#)
- Arciola, C. R., Campoccia, D., Baldassarri, L., Donati, M. E., Pirini, V., Gamberini, S., & Montanaro, L. (2006). Detection of biofilm formation in *Staphylococcus epidermidis* from implant infections. Comparison of a PCR-method that recognizes the presence of *ica* genes with two classic phenotypic methods. *Journal of Biomedical Materials Research. Part A*, 76(2), 425–430. [\[CrossRef\]](#)
- Avci, T., & Elmas, M. (2014). Milk and Blood Pharmacokinetics of Tylosin and tilimicosin following parenteral Administrations to Cows. *The Scientific World Journal*, 2014, 869096. [\[CrossRef\]](#)
- Burmayan, A., & Brundage, C. M. (2021). Caseous lymphadenitis outbreak in a small ruminant herd. *Open Veterinary Journal*, 11(4), 530–534. [\[CrossRef\]](#)
- Christensen, G. D., Simpson, W. A., Younger, J. J., Baddour, L. M., Barrett, F. F., Melton, D. M., & Beachey, E. H. (1985). Adherence of coagulase-negative staphylococci to plastic tissue culture plates: A quantitative model for the adherence of staphylococci to medical devices. *Journal of Clinical Microbiology*, 22(6), 996–1006. [\[CrossRef\]](#)
- Corrêa, J. I., Stocker, A., Trindade, S. C., Vale, V., Brito, T., Bastos, B., Raynal, J. T., de Miranda, P. M., de Alcantara, A. C., Freire, S. M., Costa, L. M., & Meyer, R. (2018). In vivo and in vitro expression of five genes involved in *Corynebacterium pseudotuberculosis* virulence. *AMB Express*, 8(1), 89. [\[CrossRef\]](#)
- de Pinho, R. B., de Oliveira Silva, M. T., Bezerra, F. S. B., & Borsuk, S. (2021). Vaccines for caseous lymphadenitis: Up-to-date and forward-looking strategies. *Applied Microbiology and Biotechnology*, 105(6), 2287–2296. [\[CrossRef\]](#)
- de Sá Guimarães, A., do Carmo, F. B., Pauletti, R. B., Seyffert, N., Ribeiro, D., Lage, A. P., Heinemann, M. B., Miyoshi, A., Azevedo, V., & Guimarães Gouveia, A. M. (2011). Caseous lymphadenitis: Epidemiology, diagnosis, and control. *IIOAB Journal*, 2(2), 33–43.
- Dias-Souza, M. V., Soares, D. L., & dos Santos, V. L. (2017). Comparative study of free and liposome-entrapped chloramphenicol against biofilms of potentially pathogenic bacteria isolated from cooling towers. *Saudi Pharmaceutical Journal*, 25(7), 999–1004. [\[CrossRef\]](#)
- Drulis-Kawa, Z., & Dorotkiewicz-Jach, A. (2010). Liposomes as delivery systems for antibiotics. *International Journal of Pharmaceutics*, 387(1–2), 187–198. [\[CrossRef\]](#)
- Dumaru, R., Baral, R., & Shrestha, L. B. (2019). Study of biofilm formation and antibiotic resistance pattern of gram-negative Bacilli among the clinical isolates at BPKIHS, Dharan. *BMC Research Notes*, 12(1), 38. [\[CrossRef\]](#)
- Ferreira, M., Ogren, M., Dias, J. N. R., Silva, M., Gil, S., Tavares, L., Aires-da-Silva, F., Gaspar, M. M., & Aguiar, S. I. (2021). Liposomes as antibiotic delivery systems: A promising nanotechnological strategy against antimicrobial resistance. *Molecules*, 26(7), 2047. [\[CrossRef\]](#)
- Foerster, S., Desilvestro, V., Hathaway, L. J., Althaus, C. L., & Unemo, M. (2017). A new rapid resazurin-based microdilution assay for antimicrobial susceptibility testing of *Neisseria gonorrhoeae*. *Journal of Antimicrobial Chemotherapy*, 72(7), 1961–1968. [\[CrossRef\]](#)
- Galvão, C. E., Fragoso, S. P., De Oliveira, C. E., Forner, O., Pereira, R. R. B., Soares, C. O., & Rosinha, G. M. S. (2017). Identification of new *Corynebacterium pseudotuberculosis* antigens by immunoscreening of gene expression library. *BMC Microbiology*, 17(1), 202. [\[CrossRef\]](#)
- Gaynor, M., & Mankin, A. S. (2003). Macrolide antibiotics: Binding Site, mechanism of action, resistance. *Current Topics in Medicinal Chemistry*, 3(9), 949–961. [\[CrossRef\]](#)
- Goel, S., & Mishra, P. (2018). Thymoquinone inhibits biofilm formation and has selective antibacterial activity due to ROS generation. *Applied Microbiology and Biotechnology*, 102(4), 1955–1967. [\[CrossRef\]](#)
- Guerrero, J. A. V., de Oca Jiménez, R. M., Acosta Dibarrat, J., León, F. H., Morales-Erasto, V., & Salazar, H. G. M. (2018). Isolation and molecular

- characterization of *Corynebacterium pseudotuberculosis* from sheep and goats in Mexico. *Microbial Pathogenesis*, 117, 304–309. [CrossRef]
- Gupta, A., Mumtaz, S., Li, C. H., Hussain, I., & Rotello, V. M. (2019). Combatting antibiotic-resistant bacteria using nanomaterials. *Chemical Society Reviews*, 48(2), 415–427. [CrossRef]
- Hallaj-Nezhadi, S., & Hassan, M. (2015). Nanoliposome-based antibacterial drug delivery. *Drug Delivery*, 22(5), 581–589. [CrossRef]
- Harrison, J. J., Ceri, H., Yerly, J., Stremick, C. A., Hu, Y., Martinuzzi, R., & Turner, R. J. (2006). The use of microscopy and three-dimensional visualization to evaluate the structure of microbial biofilms cultivated in the Calgary biofilm device. *Biological Procedures Online*, 8(1), 194–215. [CrossRef]
- Ji, L. W., Dong, L. L., Ji, H., Feng, X. W., Li, D., Ding, R. L., & Jiang, S. X. (2014). Comparative pharmacokinetics and bioavailability of tylosin tartrate and tylosin phosphate after a single oral and i.v. administration in chickens. *Journal of Veterinary Pharmacology and Therapeutics*, 37(3), 312–315. [CrossRef]
- Kluzek, M., Oppenheimer-Shaanan, Y., Dadosh, T., Morandi, M. I., Avinoam, O., Raanan, C., Goldsmith, M., Goldberg, R., & Klein, J. (2022). Designer liposomal nanocarriers are effective biofilm eradicators. *ACS Nano*, 16(10), 15792–15804. [CrossRef]
- Latif, N. A. A., Abdullah, F. F. J., Othman, A. M., Rina, A., Chung, E. L. T., Zamri-Saad, M., Saharee, A. A., Haron, A. W., & Lila, M. A. M. (2015). Isolation and detection of *Corynebacterium pseudotuberculosis* in the reproductive organs and associated lymph nodes of non-pregnant does experimentally inoculated through intradermal route in chronic form. *Veterinary World*, 8(7), 924–927. [CrossRef]
- Lohsen, S., & Stephens, D. S. (2019). Current macrolide antibiotics and their mechanisms of action. In *Antibiotic drug resistance* (pp. 97–117). Wiley. [CrossRef]
- Magdy Selim, A., Atwa, S. M., El Gedawy, A. A., & Younis, E. E. (2021). Epidemiological, bacteriological and molecular studies on caseous lymphadenitis in sheep of Dakhliya, Egypt. *Animal Biotechnology*, 0(0), 1–6. [CrossRef]
- Meers, P., Neville, M., Malinin, V., Scotto, A. W., Sardaryan, G., Kurumunda, R., Mackinson, C., James, G., Fisher, S., & Perkins, W. R. (2008). Biofilm penetration, triggered release and in vivo activity of inhaled liposomal amikacin in chronic *Pseudomonas aeruginosa* lung infections. *Journal of Antimicrobial Chemotherapy*, 61(4), 859–868. [CrossRef]
- Minozzi, G., Mattiello, S., Grosso, L., Crepaldi, P., Chessa, S., & Pagnacco, G. (2017). First insights in the genetics of caseous lymphadenitis in goats. *Italian Journal of Animal Science*, 16(1), 31–38. [CrossRef]
- Moreau-Marquis, S., Stanton, B. A., & O'Toole, G. A. (2008). *Pseudomonas aeruginosa* biofilm formation in the cystic fibrosis airway. *Pulmonary Pharmacology and Therapeutics*, 21(4), 595–599. [CrossRef]
- Mulla, S., Kumar, A., & Rajdev, S. (2016). Comparison of MIC with MBEC Assay for *in Vitro* antimicrobial Susceptibility Testing in biofilm Forming Clinical Bacterial Isolates. *Advances in Microbiology*, 06(2), 73–78. [CrossRef]
- Olson, M. E., Ceri, H., Morck, D. W., Buret, A. G., & Read, R. R. (2002). Biofilm bacteria: Formation and comparative susceptibility to antibiotics. *Canadian Journal of Veterinary Research = Revue Canadienne de Recherche Veterinaire*, 66(2), 86–92.
- Poźniak, B., Tikhomirov, M., Motykiewicz-Pers, K., Bobrek, K., & Świtała, M. (2020). Allometric analysis of tylosin tartrate pharmacokinetics in growing male turkeys. *Journal of Veterinary Science*, 21(3), e35. [CrossRef]
- Qin, H., Cao, H., Zhao, Y., Zhu, C., Cheng, T., Wang, Q., Peng, X., Cheng, M., Wang, J., Jin, G., Jiang, Y., Zhang, X., Liu, X., & Chu, P. K. (2014). In vitro and in vivo anti-biofilm effects of silver nanoparticles immobilized on titanium. *Biomaterials*, 35(33), 9114–9125. [CrossRef]
- Ruiz, H., Ferrer, L. M., Ramos, J. J., Baselga, C., Alzuguren, O., Tejedor, M. T., de Miguel, R., & Lacasta, D. (2020). The relevance of caseous lymphadenitis as a cause of culling in adult sheep. *Animals: An Open Access Journal from MDPI*, 10(11), 1962. [CrossRef]
- Rukavina, Z., & Vanić, Ž. (2016). Current trends in development of liposomes for targeting bacterial biofilms. *Pharmaceutics*, 8(2), 2–26. [CrossRef]
- Sá, M. da C. A., Veschi, J. L. A., Santos, G. B., Amanso, E. S., Oliveira, S. A. S., Mota, R. A., Veneroni-Gouveia, G., & Costa, M. M. (2013). Activity of disinfectants and biofilm production of *Corynebacterium pseudotuberculosis*. *Pesquisa Veterinária Brasileira*, 33(11), 1319–1324. [CrossRef]
- Saddiqi, M. E., Abdul Kadir, A., Abdullah, F. F. J., Abu Bakar Zakaria, M. Z., & Banke, I. S. (2022). Preparation, characterization and in vitro cytotoxicity evaluation of free and liposome-encapsulated tylosin. *OpenNano*, 8, 100108. [CrossRef]
- Schlicher, J., Schmitt, S., Stevens, M. J. A., Stephan, R., & Ghielmetti, G. (2021). Molecular characterization of *Corynebacterium pseudotuberculosis* isolated over a 15-year period in Switzerland. *Veterinary Sciences*, 8(8), 151. [CrossRef]
- Scriboni, A. B., Couto, V. M., Ribeiro, L. N. M., Freires, I. A., Groppo, F. C., de Paula, E., Franz-Montan, M., & Cogo-Müller, K. (2019). Fusogenic liposomes increase the antimicrobial activity of vancomycin against *Staphylococcus aureus* biofilm. *Frontiers in Pharmacology*, 10, 1401. [CrossRef]
- Sharma, D., Misba, L., & Khan, A. U. (2019). Antibiotics versus biofilm: An emerging battleground in microbial communities. *Antimicrobial Resistance and Infection Control*, 8(1), 76. [CrossRef]
- Sherifat B, I., Abdul Kadir, A., Abdullah J, F. F., Ramanooon, S. Z., Abdul Basit, M., & Abu Bakar, M. Z. (2021). Antibiofilm activity of oxytetracycline loaded calcium carbonate aragonite loaded nanoparticle against *Corynebacterium pseudotuberculosis*. *International Journal of Pharmacology*, 17(2), 73–83. [CrossRef]
- Skogman, M. E., Vuorela, P. M., & Fallarero, A. (2016). A platform of anti-biofilm assays suited to the exploration of natural compound libraries. *Journal of Visualized Experiments: JoVE*, 118(118), 1–10. [CrossRef]
- Stanisic, D., Fregonesi, N. L., Barros, C. H. N., Pontes, J. G. M., Fulaz, S., Menezes, U. J., Nicoleti, J. L., Castro, T. L. P., Seyffert, N., Azevedo, V., Durán, N., Portela, R. W., & Tasic, L. (2018). NMR insights on nano silver post-surgical treatment of superficial caseous lymphadenitis in small ruminants. *RSC Advances*, 8(71), 40778–40786. [CrossRef]
- Thapa, R. K., Diep, D. B., & Tønnesen, H. H. (2021). Nanomedicine-based antimicrobial peptide delivery for bacterial infections: Recent advances and future prospects. *Journal of Pharmaceutical Investigation*, 51(4), 377–398. [CrossRef]
- Vanić, Ž., Rukavina, Z., Manner, S., Fallarero, A., Uzelac, L., Kralj, M., Amidžić Klarić, D., Bogdanov, A., Raffai, T., Virok, D. P., Filipović-Grčić, J., & Škalko-Basnet, N. (2019). Azithromycin-liposomes as a novel approach for localized therapy of cervicovaginal bacterial infections. *International Journal of Nanomedicine*, 14, 5957–5976. [CrossRef]
- Wang, D.-Y., van der Mei, H. C., Ren, Y., Busscher, H. J., & Shi, L. (2020). Lipid-based antimicrobial delivery-systems for the treatment of bacterial infections. *Frontiers in Chemistry*, 7, 1–15. [CrossRef]
- Washburn, K. E., Bissett, W. T., Fajt, V. R., Libal, M. C., Fosgate, G. T., Miga, J. A., & Rockey, K. M. (2009). Comparison of three treatment regimens for sheep and goats with caseous lymphadenitis. *Journal of the American Veterinary Medical Association*, 234(9), 1162–1166. [CrossRef]
- Yitagesu, E., Alemnew, E., Olani, A., Asfaw, T., & Demis, C. (2020). Survival analysis of clinical cases of caseous lymphadenitis of goats in north Shoa, Ethiopia. *Veterinary Medicine International*, 2020, 8822997. [CrossRef]
- Zhang, J., Leifer, F., Rose, S., Chun, D. Y., Thaisz, J., Herr, T., Nashed, M., Joseph, J., Perkins, W. R., & DiPetrillo, K. (2018). Amikacin liposome inhalation suspension (ALIS) penetrates non-tuberculous mycobacterial biofilms and enhances amikacin uptake into macrophages. *Frontiers in Microbiology*, 9, 915. [CrossRef]
- Zong, T. X., Silveira, A. P., Morais, J. A. V., Sampaio, M. C., Muehlmann, L. A., Zhang, J., Jiang, C. S., & Liu, S. K. (2022). Recent advances in antimicrobial nano-drug delivery systems. *Nanomaterials*, 12(11), 1855. [CrossRef]